

Supporting Information

Development of Noncovalent Small-Molecule Keap1–Nrf2 Inhibitors by Fragment-Based Drug Discovery

Dilip Narayanan,^{†,||} Kim T. Tran,^{†,||} Jakob S. Pallesen,^{†,⊥} Sara M. Ø. Solbak,^{†,⊥} Yuting Qin,^{†,⊥}
Elina Mukminova,[†] Martina Luchini,[†] Kristina O. Vasilyeva,[†] Dorleta González Chichón,[†] Georgia Goutsiou,[†] Cecilie
Poulsen,[‡] Nanna Haapanen,[†] Grzegorz M. Popowicz,^{¥,‡} Michael Sattler,^{¥,‡} David Olnagier,[‡] Michael Gajhede,[†]
Anders Bach^{†,*}

[†]Department of Drug Design and Pharmacology, Faculty of Health and Medical Sciences, University of
Copenhagen, Universitetsparken 2, 2100 Copenhagen, Denmark

[‡]Department of Biomedicine, Faculty of Health, Aarhus University, 8000 Aarhus C, Denmark

[¥]Institute of Structural Biology, Helmholtz Zentrum München, 85764 Neuherberg, Germany

[‡]Bavarian NMR Center, Department of Chemistry, Technical University of Munich, 85747 Garching, Germany

*E-mail: anders.bach@sund.ku.dk

Contents

Supporting Tables	S2
Table S1. PDB structures—X-ray crystallographic data and refinement statistics. ^a	S2
Supporting Figures	S4
Figure S1. X-ray crystal structures of category 1 and 2 fragment hits.....	S4
Figure S2. SPR sensorgrams of initial analogues.....	S5
Figure S3. X-ray crystal structures of compound 67 and 77 (including electron densities).	S7
Figure S4. Chiral HPLC of racemic 118 to pure enantiomers 119 and 120 and molecular docking.....	S8
Figure S5. SPR sensorgrams of lead compounds.	S9
Figure S6. Binding mode of compound 119 compared to known Keap1 inhibitors.	S10
Figure S7. LCMS traces (UV254) of key compounds	S11

Supporting Tables

Table S1. PDB structures—X-ray crystallographic data and refinement statistics.^a

PDB ID	7OF8	7OF9	7OFA	7OFB	7OFC	7OFD	7OFE	7OFF
Synchrotron Beamline	ESRF-ID29	ESRF-ID29	ESRF-ID29	ESRF-ID29	ESRF-ID23-1	PETRA-P13	PETRA-P14	Bio-MAX
Wavelength [Å]	0.9772	0.9772	0.9772	1.0723	0.9763	0.9762	0.9791	0.9763
Resolution range [Å]	38.16 - 1.78 (1.84 - 1.78)	52.17 - 1.80 (1.86 - 1.80)	51.75 - 2.22 (2.3 - 2.22)	47.16 - 2.40 (2.49 - 2.4)	51.58 - 1.97 (2.04 - 1.97)	51.51 - 1.25 (1.29 - 1.24)	37.67 - 1.19 (1.23 - 1.19)	51.59 - 1.37 (1.42 - 1.37)
Space group	P 61	P 61	P 61	P 61	P 61	P 61	P 61	P 61
Unit cell: a, b, c [Å] α, β, γ [°]	104.32, 104.32, 55.99 90, 90, 120	104.34, 104.34, 56.03 90, 90, 120	103.51, 103.51, 55.75 90, 90, 120	103.36, 103.36, 55.49 90, 90, 120	103.16, 103.16, 55.58 90, 90, 120	103.01, 103.01, 55.03 90, 90, 120	103.08, 103.08, 55.20 90, 90, 120	103.19, 103.19, 55.6 90, 90, 120
Total reflections	443,863 (32,408)	435,941 (35,494)	277,235 (2,6008)	89,979 (8,867)	340,627 (33,914)	1,662,590 (73,253)	1,427,274 (107,126)	1,277,321 (70,329)
Unique reflections	33,483 (3,311)	32,391 (3,207)	16,965 (1,696)	13,361 (1,308)	24,108 (2,375)	91,534 (8,560)	106,493 (10,446)	71,319 (7,092)
Multiplicity	13.3 (9.8)	13.5 (11.1)	16.3 (13.6)	6.7 (6.8)	14.1 (14.3)	18.2 (8.6)	13.4 (10.3)	17.9 (9.9)
Completeness (%)	99.7 (99.3)	99.5 (99.7)	99.9 (99.00)	99.9 (99.7)	99.9 (100.0)	99.2 (93.3)	99.8 (98.6)	99.9 (99.9)
Mean I/sigma(I)	11.12 (2.12)	10.87 (2.22)	8.07 (2.30)	14.55 (4.27)	15.28 (2.25)	24.73 (2.45)	23.41 (3.81)	21.56 (2.09)
Wilson B-factor	26.76	27.87	35.91	36.59	31.96	14.23	12.49	14.96
R-merge	0.124 (0.810)	0.124 (0.856)	0.236 (0.869)	0.079 (0.34)	0.104 (1.080)	0.061 (0.598)	0.060 (0.707)	0.096 (1.328)
R-meas	0.129 (0.856)	0.129 (0.898)	0.243 (0.906)	0.086 (0.363)	0.107 (1.119)	0.062 (0.638)	0.062 (0.745)	0.098 (1.4)
R-pim	0.035 (0.271)	0.035 (0.267)	0.060 (0.246)	0.033 (0.139)	0.028 (0.294)	0.014 (0.215)	0.017 (0.233)	0.022 (0.433)
CC1/2	0.99 (0.63)	0.99 (0.60)	0.99 (0.97)	0.99 (0.98)	0.99 (0.85)	1 (0.88)	0.99 (0.88)	1 (0.85)
CC*	0.99 (0.88)	1 (0.86)	0.99 (0.99)	0.999 (0.99)	1 (0.96)	1 (0.97)	1 (0.97)	1 (0.96)
Reflections used in refinement	33,482 (3,310)	32,390 (3,207)	16,965 (1,679)	13,361 (1,305)	24,107 (2,375)	91,456 (8,559)	106,489 (10,448)	71,318 (7,087)
Reflections used for R-free	1,628 (170)	1,703 (143)	813 (81)	666 (66)	1,231 (122)	4,573 (423)	5,326 (523)	3,557 (386)
R-work	0.188 (0.325)	0.201 (0.354)	0.209 (0.390)	0.19 (0.29)	0.191 (0.254)	0.150 (0.200)	0.130 (0.165)	0.150 (0.208)
R-free	0.224 (0.345)	0.225 (0.358)	0.242 (0.410)	0.225 (0.266)	0.210 (0.298)	0.171 (0.249)	0.150 (0.202)	0.173 (0.242)
CC(work)	0.970 (0.772)	0.963 (0.723)	0.823 (0.078)	0.959 (0.924)	0.954 (0.909)	0.968 (0.939)	0.969 (0.925)	0.969 (0.935)
CC(free)	0.955 (0.789)	0.961 (0.780)	0.938 (0.666)	0.942 (0.909)	0.966 (0.842)	0.959 (0.893)	0.959 (0.876)	0.962 (0.913)
Number of non-hydrogen atoms	2,329	2,332	2,246	2,272	2,337	2,581	2,655	2,521
Number of atoms in macromolecules	2,216	2,216	2,222	2,219	2,235	2,326	2,339	2,292

Number of atoms in ligands	16	15	16	50	40	67	59	73
Number of solvent molecules	97	101	8	3	62	188	257	156
Number of protein residues	288	288	289	289	289	291	291	291
RMS(bonds) [Å]	0.015	0.005	0.004	0.005	0.007	0.007	0.007	0.008
RMS(angles) [°]	1.49	1.05	0.99	1.08	1.13	1.33	1.34	1.31
Ramachandran favored (%)	97.20	96.50	95.12	96.52	97.56	96.89	96.54	96.89
Ramachandran allowed (%)	2.80	3.50	4.88	3.48	2.44	3.11	3.46	3.11
Ramachandran outliers (%)	0.00	0.00	0.00	0.00	0.00	0.00	0.00	0.00
Rotamer outliers (%)	0.42	0.00	0.42	0.42	0.00	0.00	0.00	0.00
Clashscore	2.31	2.54	1.84	2.72	2.94	4.49	2.99	1.96
Average B-factor [Å ²]	40.28	37.83	44.14	46.39	41.08	18.82	18.42	20.35
Average B-factor macromolecules [Å ²]	40.11	37.64	44.12	45.87	40.62	17.73	16.52	19.48
Average B-factor ligands [Å ²]	65.14	71.54	50.34	69.70	73.31	37.44	37.32	34.58
Average B-factor solvent [Å ²]	39.97	37.03	35.74	42.25	36.84	25.71	31.39	26.39
Number of TLS groups	8	0	0	7	0	0	0	0
Ligand ID	VCQ	VBK	VBT	VCN	VCT	VBW	VBQ	VCB
Ligand CC	0.87	0.75	0.95	0.63	0.64	0.86	0.84	0.97

^a Statistics for the highest-resolution shell are shown in parentheses.

Supporting Figures

Figure S1. X-ray crystal structures of category 1 and 2 fragment hits.

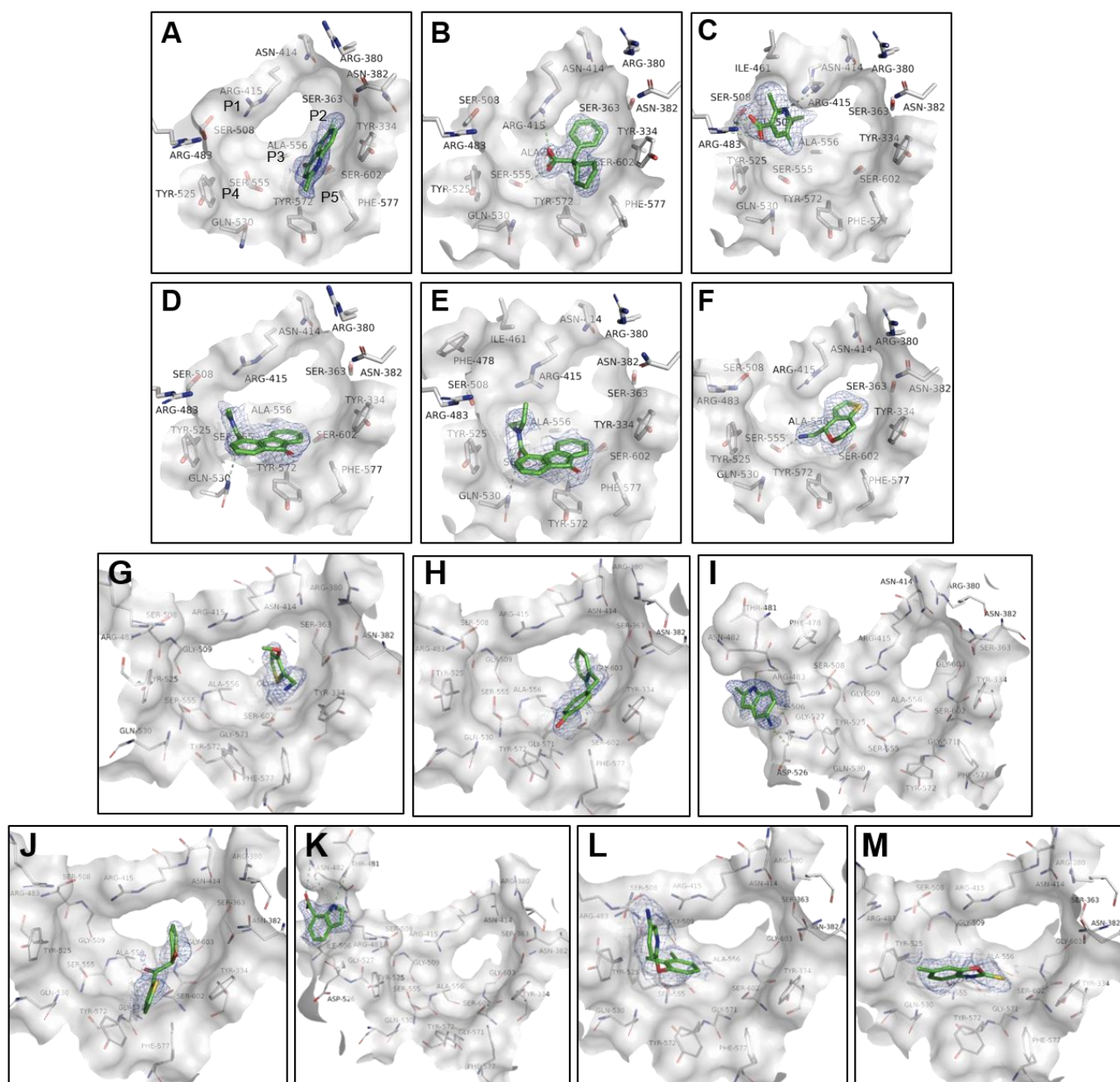
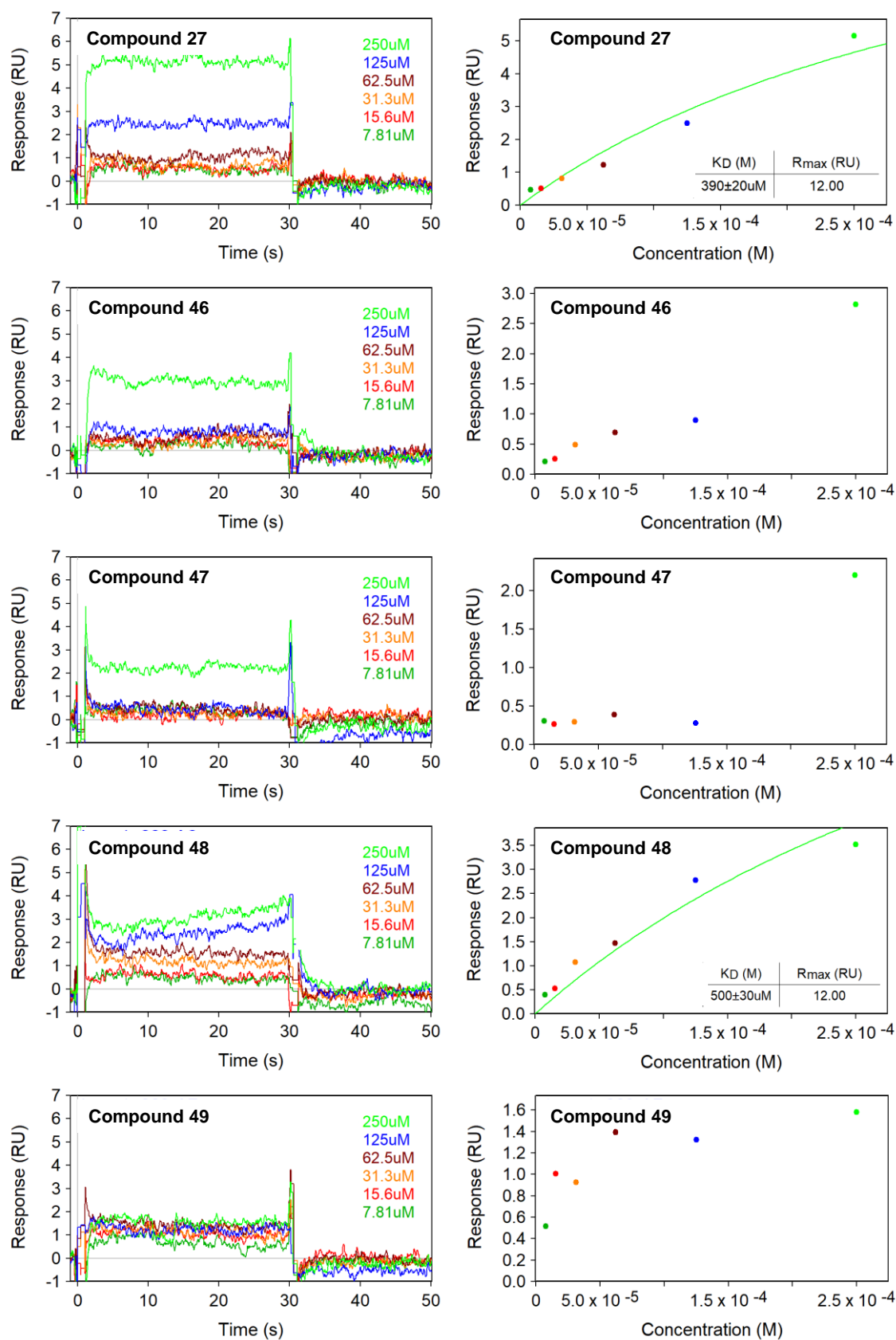


Figure S1. (A–F) X-ray crystal structures of the category 1 fragment hits **18** (PDB ID: 7OFD), **36** (PDB ID: 7OF8), **37** (PDB ID: 7OFA), **43** (PDB ID: 7OFC), **44** (PDB ID: 7OFB) and **45** (PDB ID: 7OF9) (green), respectively, in complex with the Keap1 Kelch domain (grey) with indication of the P1–5 subpockets (A). (G–M) X-ray crystal structures of the category 2 fragment hits **20**, **23**, **24**, **25**, **26**, **39**, and **41**, respectively, in complex with the Keap1 Kelch domain. (A–M) Standard $2F_o - F_c$ electron density map carved around the fragments at 1.6 Å (blue) contoured at 0.5 σ are shown (in contrast to **Figure 3**, where $\sigma=1$).

Figure S2. SPR sensorgrams of initial analogues.



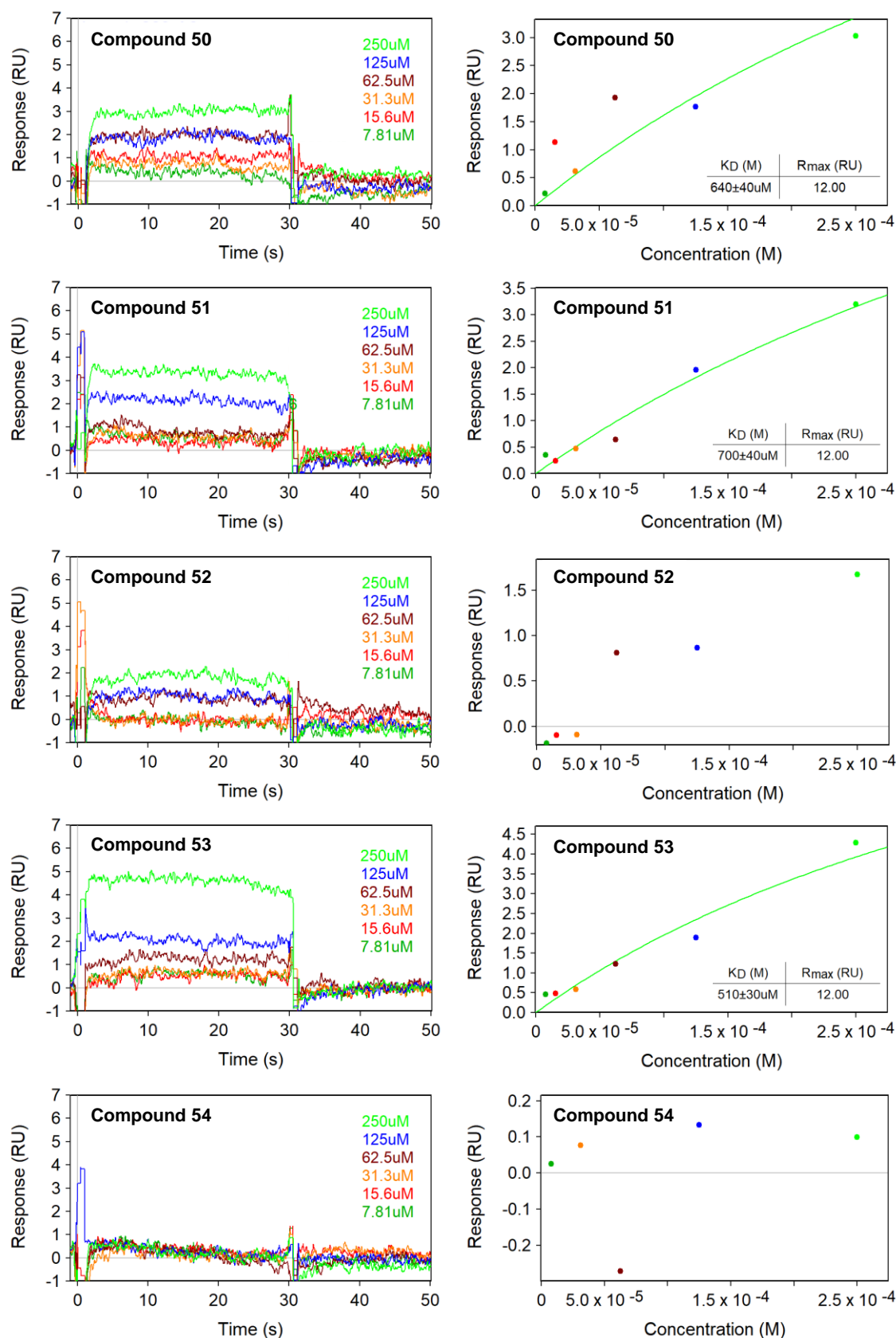


Figure S2. SPR sensorgrams of initial analogues of the fluorenone carboxamide fragments **27**, **43**, and **44**. The analogues were tested by dose-response fixed-concentration injections in twofold serial dilutions (7–250 μ M; $n = 1$) (left panels). K_d values were estimated from steady-state affinity analysis by fitting to a 1:1 model and by fixing R_{max} to the value of the control peptide (H-LDEETGEFL-OH) (right panels).

Figure S3. X-ray crystal structures of compound 67 and 77 (including electron densities).

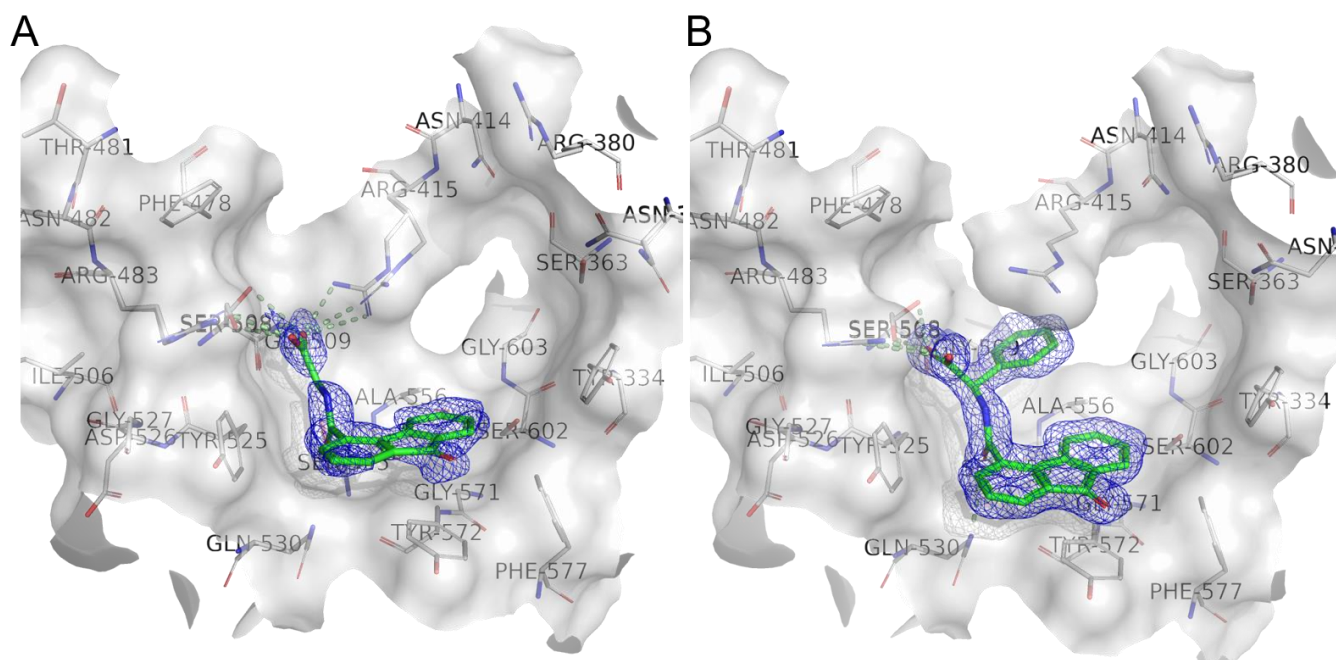


Figure S3. (A-B) X-ray crystal structures of compound **67** (A) and **77** (B) (PDB ID: 7OFE and 7OFF, respectively) in complex with the Keap1 Kelch domain (grey). Standard 2Fo - Fc electron density map carved around the compounds at 1.6 Å (blue) contoured at 1σ are shown.

Figure S4. Chiral HPLC of racemic 118 to pure enantiomers 119 and 120 and molecular docking.

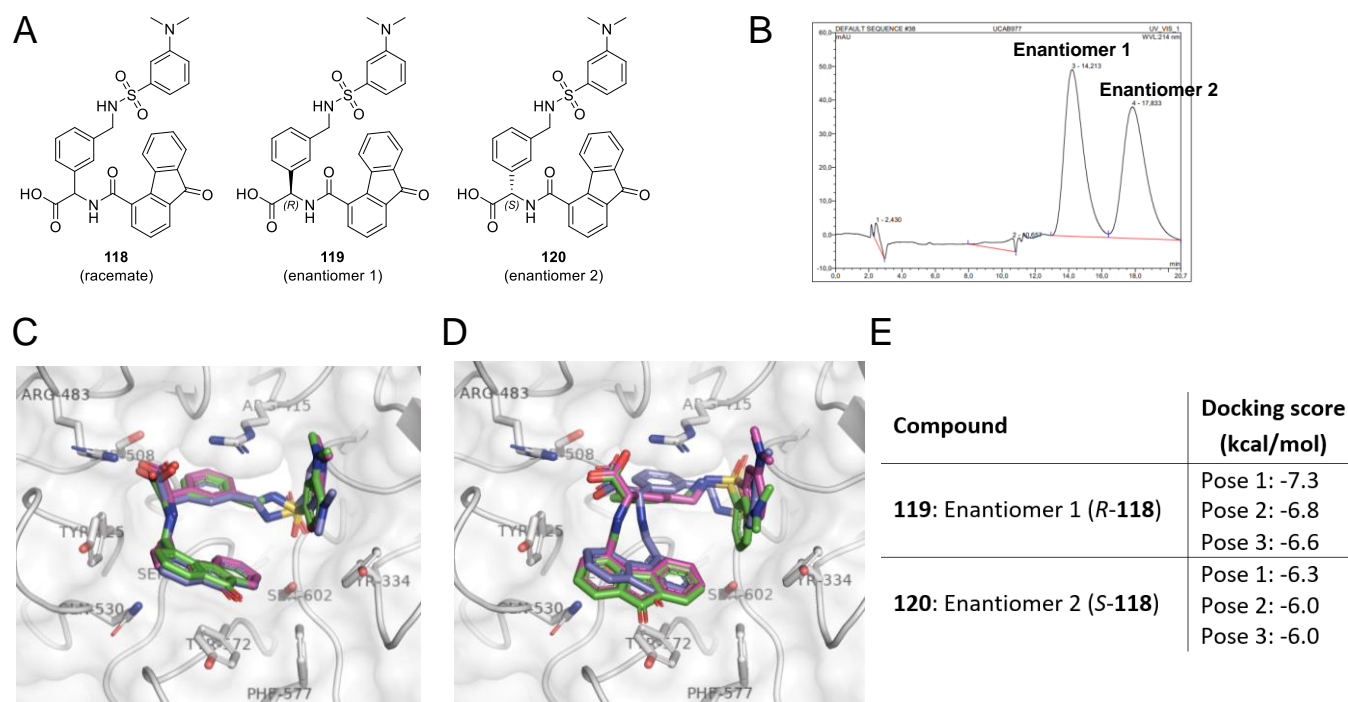


Figure S4. (A–B) Chiral separation of **118** into pure enantiomer 1 (**119**) and 2 (**120**) was performed using a Chiralcel OD column. Two runs were performed, where 7.0 and 7.2 mg of **118** were solubilized in EtOH:heptane 50:50 v/v% to a concentration of 1 mg/mL and loaded on the column. The two enantiomers were completely separated by isocratic elution using EtOH:heptane:TFA 30:70:0.1 v/v%. The fractions of the pure enantiomers were evaporated, resolubilized in MeCN:water 1:1 v/v% and freeze-dried, resolubilized in DMSO- d_6 , and characterized by LC–MS and qHNMR. (C–E) Molecular docking of **119** (C) and **120** (D) together with affinities in the FP assay (**Table 4**) indicate that enantiomer 1 (**119**) and enantiomer 2 (**120**) are the *R*- and *S*-form of **118**, respectively. **119** is 22-fold more potent than **120** in FP, and its top 3 highest-scoring docking poses show less variability (C) and have better scores (E) compared to **120** (D and E). Top 3 poses are shown in green (pose 1), magenta (pose 2), and blue (pose 3).

Figure S5. SPR sensorgrams of lead compounds.

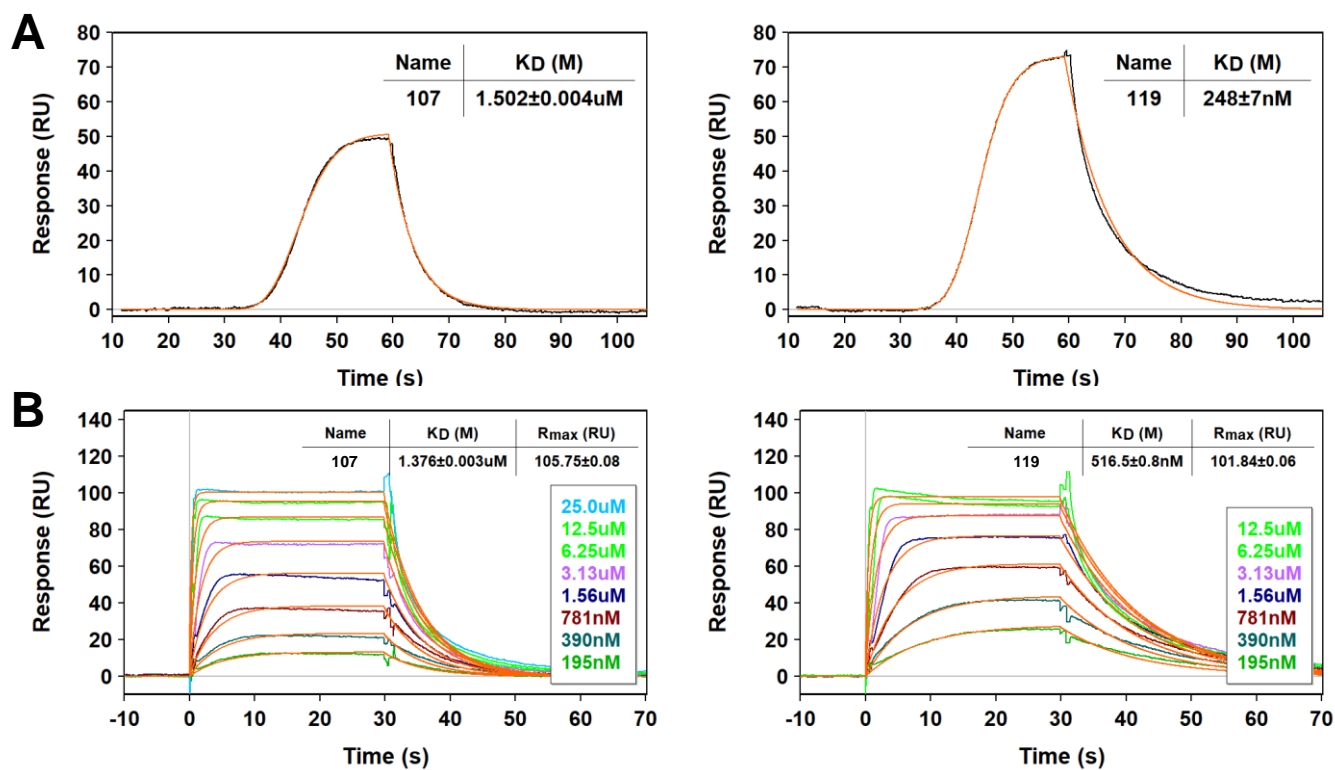


Figure S5. SPR sensorgrams of **107** and **119** binding to immobilized Keap1 Kelch domain. The compounds were tested by OneStep gradient injections (1 μM) (A) and dose-response fixed-concentration injections in twofold serial dilutions (B). K_d values were determined by kinetic fitting of the SPR sensorgrams to a 1:1 interaction model.

Figure S6. Binding mode of compound 119 compared to known Keap1 inhibitors.

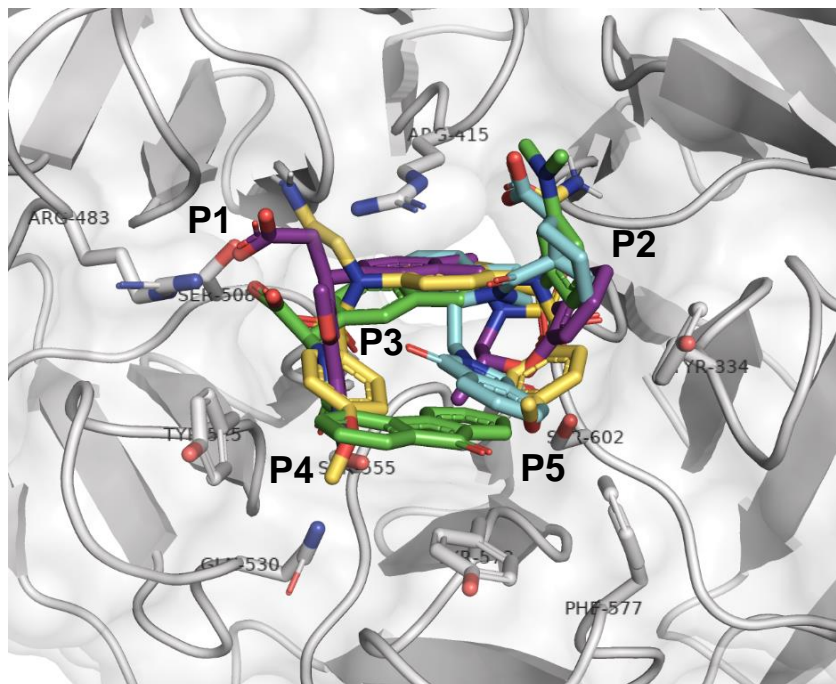
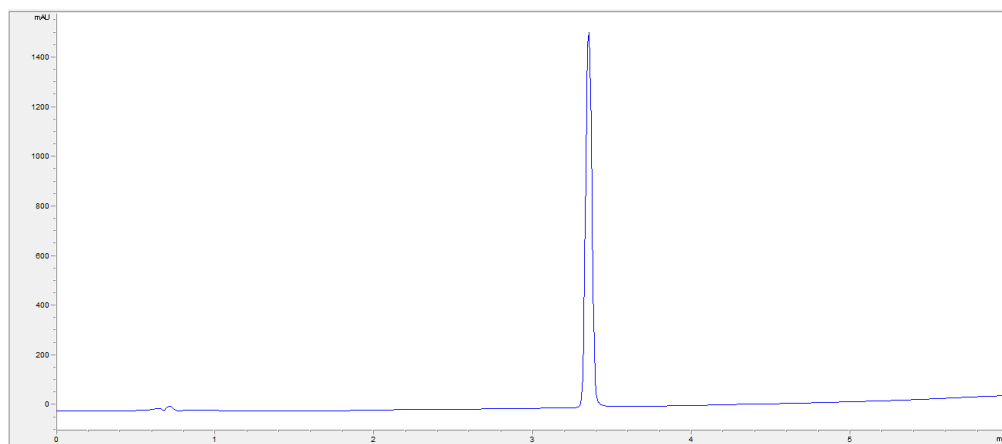


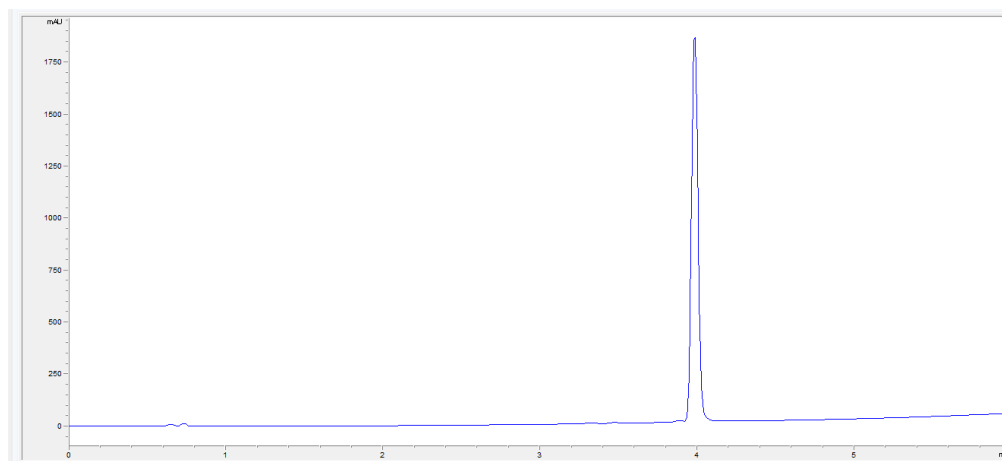
Figure S6. Aligned structures of compounds in complex with the Keap1 Kelch domain (grey) including indication of the P1–5 subpockets. Compounds shown: **119** (pose 1 from molecular docking, green), **1** (PDB ID 4L7B, cyan), **4** (PDB ID 4XMB, yellow), and **7** (PDB ID 5FNU, purple).

Figure S7. LCMS traces (UV254) of key compounds

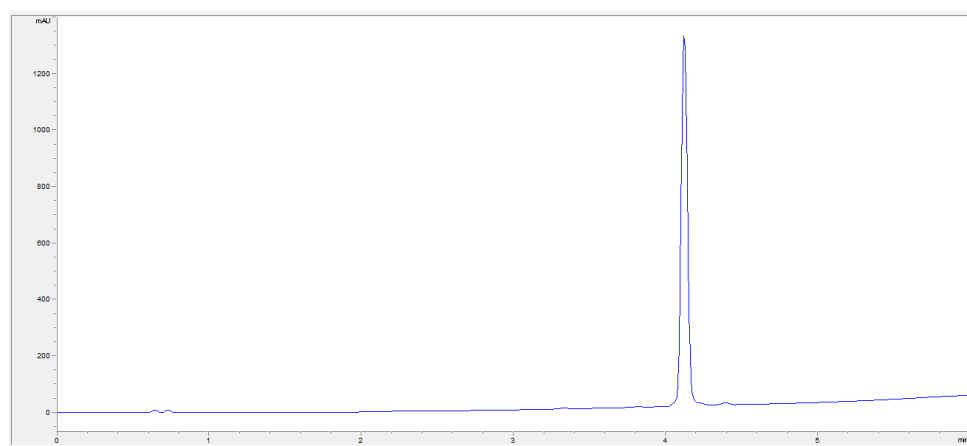
Compound 67



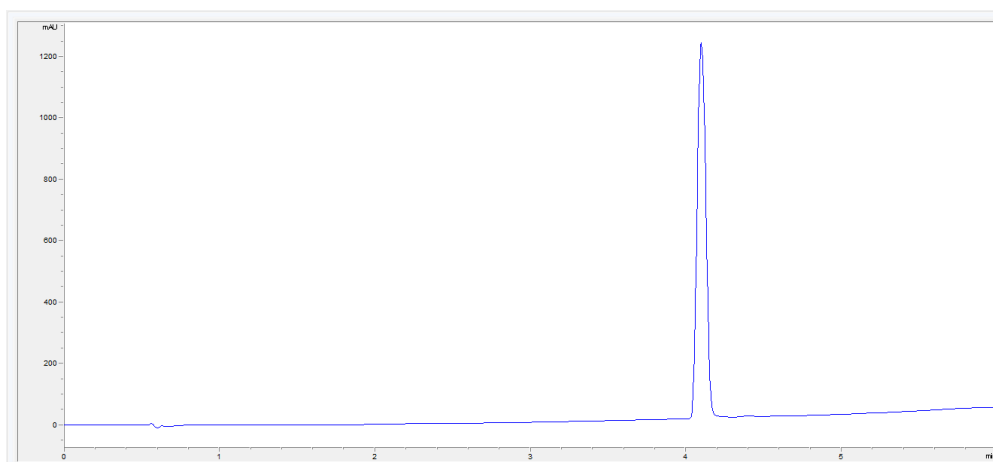
Compound 77



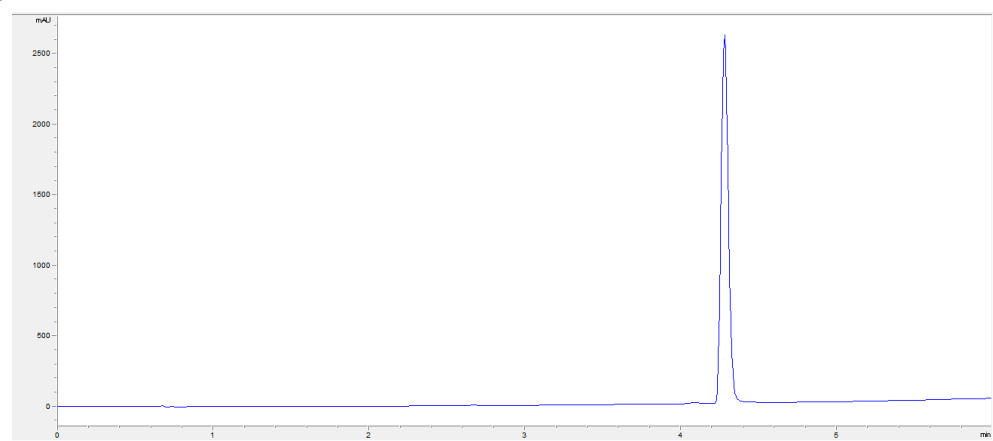
Compound 104



Compound 107



Compound 118



Compound 119

